

1 **Electronic Supplementary Information for**  
2 **A Dual-Responsive Microemulsion with**  
3 **Macroscale Superlubricity and Largely Switchable**  
4 **Friction**

5 Siwei Chen,<sup>a,b</sup> Hong Sun,<sup>c</sup> Jian Liu,<sup>a</sup> Jinyu Wang,<sup>b</sup> Hongsheng Lu,<sup>b</sup> Jingcheng Hao,<sup>\*d,e</sup> Lu  
6 Xu<sup>\*a,e</sup> and Weimin Liu<sup>a,e</sup>

7 <sup>a</sup> State Key Laboratory of Solid Lubrication, Lanzhou Institute of Chemical Physics, Chinese  
8 Academy of Sciences, Lanzhou 730000, China

9 <sup>b</sup> College of Chemistry and Chemical Engineering, Southwest Petroleum University, Chengdu  
10 610500, China

11 <sup>c</sup> School of Chemistry and Pharmaceutical Engineering, Shandong First Medical University &  
12 Shandong Academy of Medical Sciences, Tai'an 271016, China

13 <sup>d</sup> Key Laboratory of Colloid and Interface Chemistry & Key Laboratory of Special  
14 Aggregated Materials (Ministry of Education), Shandong University, Jinan 250100, China

15 <sup>e</sup> Shandong Laboratory of Advanced Materials and Green Manufacturing at Yantai, Yantai  
16 264006, China

17 \*E-mail: [jhao@sdu.edu.cn](mailto:jhao@sdu.edu.cn); [xulu@licp.cas.cn](mailto:xulu@licp.cas.cn).

18

## 19 **S1: Experimental Section**

### 20 **Synthesis of Cationic Emulsifiers**

21 Materials for preparing magnetic cationic emulsifiers including didodecyldimethylammonium  
22 chloride (DDACl), cerous chloride ( $\text{CeCl}_3$ ), ferric chloride ( $\text{FeCl}_3$ ) and gadolinium chloride  
23 ( $\text{GdCl}_3$ ) were purchased from Aladdin Biochemical Technology Co. Ltd., China. All the  
24 chemicals have a purity above 98% and were used as sources. Magnetic cationic surfactants  
25 didodecyldimethylammonium tetrachloroacetate (DDACe), didodecyldimethyl-ammonium  
26 tetrachloroferrate (DDAFe) and didodecyldimethylammonium tetrachlorogadolate (DDAGd)  
27 were synthesized by mixing an equal molar amount of DDABr with  $\text{CeCl}_3$ ,  $\text{FeCl}_3$  and  $\text{GdCl}_3$ ,  
28 respectively, in methanol and stirring overnight at room temperature.<sup>1,2</sup> The solvents were then  
29 evaporated and the products were dried under reduced pressure at 80 °C overnight, yielding  
30 white, orange and white solids for DDACe, DDAFe and DDAGd, respectively.

### 31 **Sample Preparation**

32 Aqueous solutions of different cationic surfactants were mixed with EG and an equal volume  
33 of n-hexane at desired amounts and stoichiometric ratios in glass serum bottles at room  
34 temperature. The mixtures were stirred at 2500 rpm for 10 min to achieve homogenization. All  
35 the samples were kept at  $20 \pm 0.5$  °C and their phase behaviour was recorded after one-month  
36 storage. Both the oil and glycol were received from Sinopharm Chemical Reagent Co. Ltd.,  
37 China and have a purity  $\geq 99\%$ . Ultrapure water ( $\rho = 18.25$  m $\Omega$ ·cm) was employed to prepare  
38 all the sample solutions and microemulsions (MEM).

### 39 **Sample Characterizations**

40 Electrical conductivity measurements for obtaining the cmc and  $\beta$  of cationic surfactants as well  
41 as the conductivity of a MEM were carried out using a DDS-307A analyzer. The magnetism of  
42 different cationic surfactants was characterized by a MPMSXL SQUID magnetometry  
43 (Quantum Design, USA). The type of various MEM was determined using drop tests after

44 stained with a hydrophilic dye methylene blue. The internal size distribution and zeta potential  
45 of different MEM and emulsions (EM) were analysed by a Nano ZS90 potential analyser  
46 (Malvern, UK) equipping with parallel-plate platinum black electrodes spaced 5 mm apart and  
47 a 10 mm path-length rectangular organic glass cell. The interfacial tension of DDACe and  
48 DDACe/EG mixture at the n-hexane/water interface at different temperatures was examined by  
49 a TX-500C spinning drop interface tensiometer (CNG, USA). The freezing point of n-hexane,  
50 DDACe MEM and aqueous solutions of DDACe and EG was measured using a DSC 204  
51 differential scanning calorimeter (NATZSCH, Germany) at a cooling rate of 5 °C min<sup>-1</sup>.

## 52 **Friction and Wear Tests**

53 The tribological performance of different MEM and EM were determined by a friction and wear  
54 tester designed and constructed by Lanzhou Institute of Chemical Physics using a sliding ball-  
55 on-disc configuration with steel ball (AISI 52100, Diameter: 3 mm, Hardness: 61-65 HRC) and  
56 substrate (AISI 52100, Diameter: 24 mm, Thickness: 8 mm, Hardness: 61-65 HRC, Roughness  
57 ( $R_a$ ): 13 nm) as counterparts.<sup>3, 4</sup> Both the ball and substrate had been cleaned ultrasonically in  
58 petroleum ether and methanol before the measurements. The testing temperature range was  
59 between -60 and 60 °C, the sliding velocity range was set to be between 0.005 and 0.5 m s<sup>-1</sup>,  
60 the applied normal loads were 2, 4, 6, 8 and 10 N, corresponding to average effective contact  
61 normal pressures of 1.4, 1.6, 1.8, 2.0 and 2.2 GPa, respectively, the testing time was 30 min.  
62 All the measurements were repeated for at least three times to ensure a reproducibility, the  
63 average CoF values were calculated from multiple reproducible measurements. In each  
64 measurement, the environmental temperature was rigorously maintained at a target value of  
65  $\pm 0.5$  °C using an electrothermostatic controller to avoid any possible temperature variations  
66 from the friction between two contacting steel surfaces. The switchable frictional behaviour of  
67 the DDACe/n-hexane/water/EG mixture was tested by alternately varying system temperatures  
68 between 20 and 50 °C *in situ* for closely simulating the scenario in practical applications where  
69 the temperature usually changes in real-time.

70 The wear volume of a steel disc after the frictional tests was determined using a  
71 MicroXAM 800 3D surface profiler (KLA-Tencor, USA). The wear tracks on steel substrates  
72 after lubricated with different materials were characterized by a JSM-7610 field emission SEM  
73 (JEOL, Japan), a MicroXAM 800 3D surface profiler (KLA-Tencor, USA) and an Axioscope  
74 5 optical microscopy (OM, Zeiss, Germany), respectively. The tribochemical reactions of a  
75 DDACe MEM or EM during the lubrication process were examined by a K-Alpha XPS  
76 (Thermo Scientific, USA). The ECR of n-hexane, water, EG, DDACe solution and the  
77 DDACe/EG/n-hexane/water mixture at 20 and 50 °C was measured by an SRV-IV oscillating  
78 friction and wear tester (Optimol, Germany).

### 79 **Molecular Dynamics Simulations**

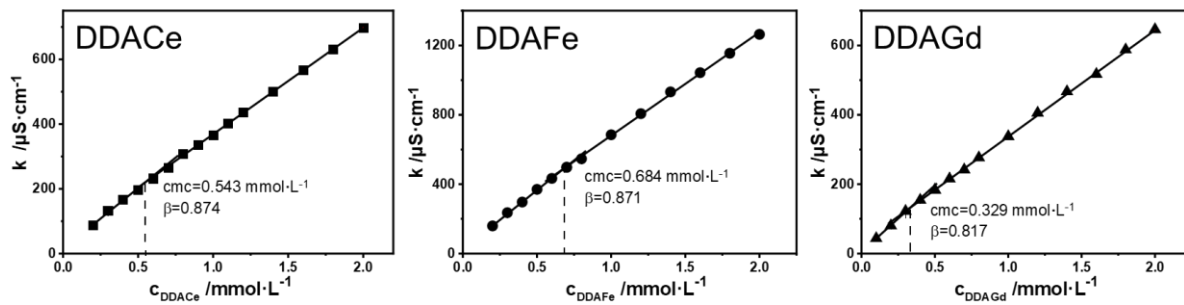
80 Classical molecular dynamics (MD) simulations were implemented by creating a MD box with  
81 dimensions of  $40 \times 40 \times 160 \text{ \AA}^3$ , where Fe substrates with a thickness of  $\sim 20 \text{ \AA}$  and (100)  
82 surface was placed at the bottom of the box while a mixture of 1000 EG molecules, 40  $\text{DDA}^+$   
83 and 40  $[\text{CeCl}_4]^-$  ions was placed above the Fe substrate. Periodic boundary conditions were  
84 imposed on the two orthogonal (*i.e.*,  $x$  and  $y$ ) directions to mimic infinite planar iron substrate  
85 and a wall-boundary condition was exerted on the out-of-plane direction. Polymer Consistent  
86 Force Field (PCFF) was used to describe the atomic interactions with atomic partial charges of  
87 the EG/DDA<sup>+</sup>/[CeCl<sub>4</sub>]<sup>-</sup> mixture assigned according to the QEq charge.<sup>5</sup> For the non-bonded  
88 atomic interactions, 12-6 Lennard-Jones (LJ) potential with a cutoff distance of 10.0 Å was  
89 applied to describe the van der Waals forces between atoms, whereas standard Coulomb  
90 potential was employed to mimic the electrostatic interactions evaluated with the particle-  
91 particle particle-mesh (PPPM) algorithm. For the Ce atom in the [CeCl<sub>4</sub>]<sup>-</sup> ion, the 126- LJ  
92 parameters were taken from a recent study by Kanhaiya et al..<sup>6</sup>

93 Specifically, energy minimizations were firstly conducted to relax the system with an  
94 energy and force tolerances of 0.00001 Kcal mol<sup>-1</sup> and 0.00001 Kcal mol<sup>-1</sup> Å<sup>-1</sup>, respectively.  
95 Then MD simulations with 100,000 timesteps were carried out to further relax the systems

96 under canonical ensemble at temperatures of 20 and 50 °C. At last, MD simulations with  
97 10,000,000 timesteps were performed to capture the structural properties of the  
98 EG/DDA<sup>+</sup>/[CeCl<sub>4</sub>]<sup>-</sup> mixture that was in contact with the Fe substrate. During the whole  
99 simulation process, the movement of atoms was controlled by the classical Newton's motion,  
100 in which the velocity-Verlet algorithm with a timestep of 1.0 fs was applied to integrate the  
101 classic Newton's equation. The temperature was controlled by the Nose-hoover thermostat.

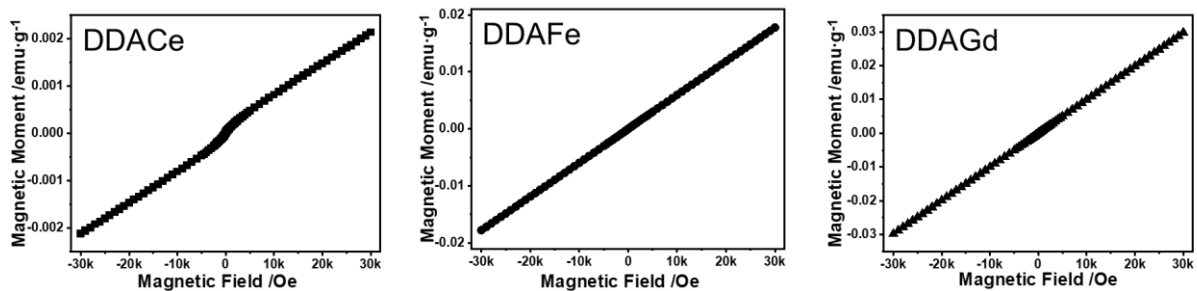
102

103 **S2: Supplementary Figures and Tables**

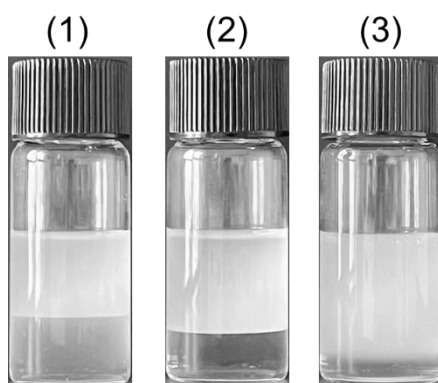


104  
105 **Figure S1.** Electrical conductivity measurements of surfactant DDACe, DDAFe and DDAGd.  
106  $T = 20\text{ }^\circ\text{C}$ .

107



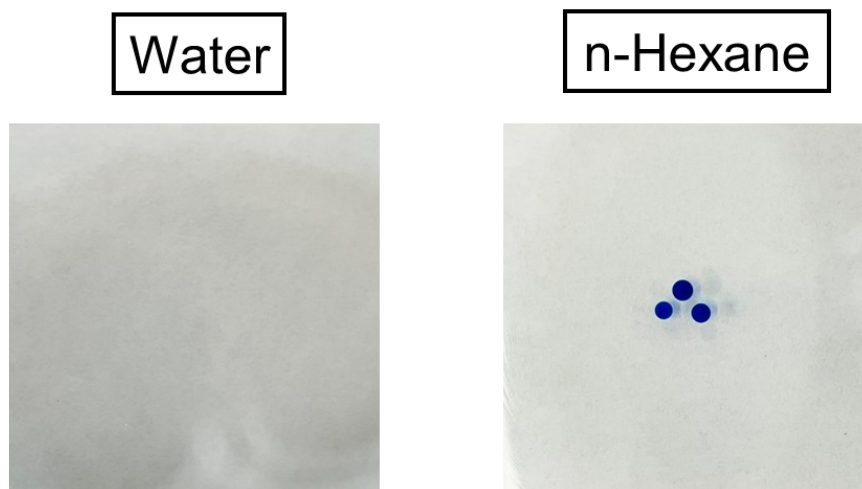
108  
 109 **Figure S2.** SQUID magnetometry results of DDACe, DDAFe and DDAGd. T = 20 °C. The  
 110 magnetic moment generally followed a linear relationship with the strength of an applied  
 111 magnetic field, indicative of a paramagnetic nature of the three kinds of surfactants.<sup>1,2</sup>  
 112



113  
114 **Figure S3.** Photographs of turbid EM formed by the DDACe/EG/water/n-hexane mixture at  
115 different stoichiometric ratios: (1) 47.78 wt% DDACe solution, 13.18 wt% EG, 39.04 wt% n-  
116 hexane; (2) 37.42 wt% DDACe solution, 13.75 wt% EG, 48.83 wt% n-hexane; (3) 16.84 wt%  
117 DDACe solution, 12.07 wt% EG, 71.09 wt% n-hexane. T = 20 °C.

118



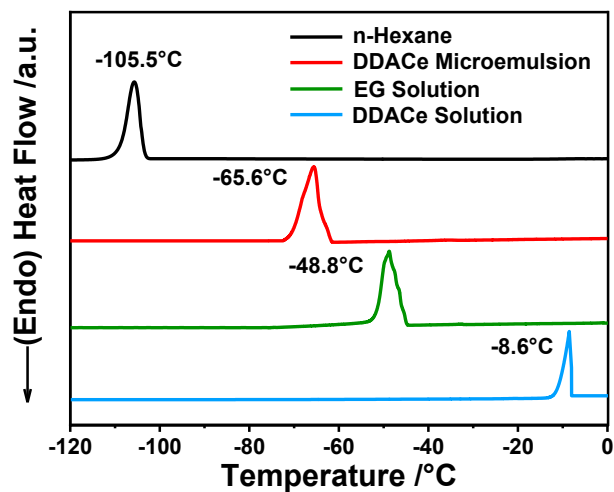


119

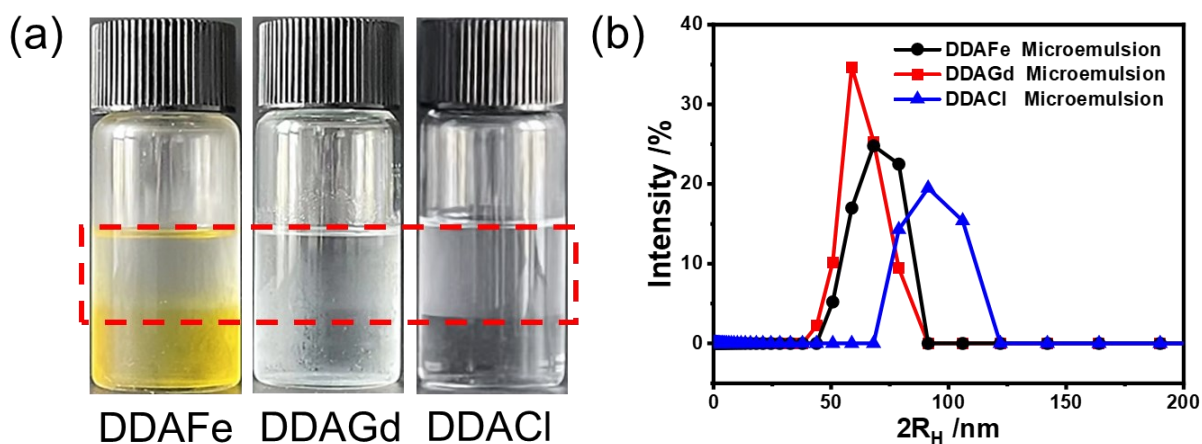
120 **Figure S4.** Photographs of  $\sim 5 \mu\text{L}$  DDACe MEM droplets (stained with methylene blue) after

121 added into water and n-hexane, respectively.  $T = 20 \text{ }^\circ\text{C}$ .

122



123  
 124 **Figure S5.** Differential scanning calorimetry (DSC) spectra of n-hexane, 15 mmol L<sup>-1</sup> DDACe  
 125 and 40 wt% EG solutions, and a MEM consisting of 35.43 wt% DDACe solution, 26.03 wt%  
 126 EG and 38.54 wt% n-hexane, a surfactant concentration of 15 mmol L<sup>-1</sup> and a volume ratio of  
 127 water-to-oil = 1:1 in a temperature range between -120 and 0 °C. The results suggest an  
 128 excellent anti-freezing property of the DDACe MEM.  
 129



130  
 131 **Figure S6.** (a) Photographs and (b) internal size distribution of representative DDAFe, DDAGd  
 132 and DDACl MEM. All the MEM contained 35.43 wt% surfactant solution, 26.03 wt% EG and  
 133 38.54 wt% n-hexane. The surfactant concentration was  $15 \text{ mmol L}^{-1}$ , and the volume ratio  
 134 between the aqueous and oil phases was 1:1.  $T = 20 \text{ }^\circ\text{C}$ .  
 135

136 **Table S1.** Phase behaviour and colloidal stability of the surfactant/EG/water/n-hexane mixtures  
 137 with a constant amount of EG, water and oil ( $v:v:v = 0.36:1:1$ ) but different surfactant  
 138 concentrations at 20 °C. The results suggest a highest thermodynamic stability of the DDACe  
 139 MEM.

Concentration (mmol·L <sup>-1</sup> )	DDACe	DDAFc	DDAGd	DDACl
25×10 <sup>-3</sup>	○	○	○	○
21×10 <sup>-3</sup>	○	○	○	○
20×10 <sup>-3</sup>	●	⊙	⊙	⊙
15×10 <sup>-3</sup>	●	⊙	⊙	●
12×10 <sup>-3</sup>	●	○	●	●
11×10 <sup>-3</sup>	○	○	○	○
5×10 <sup>-3</sup>	○	○	○	○
0×10 <sup>-3</sup>	×	×	×	×

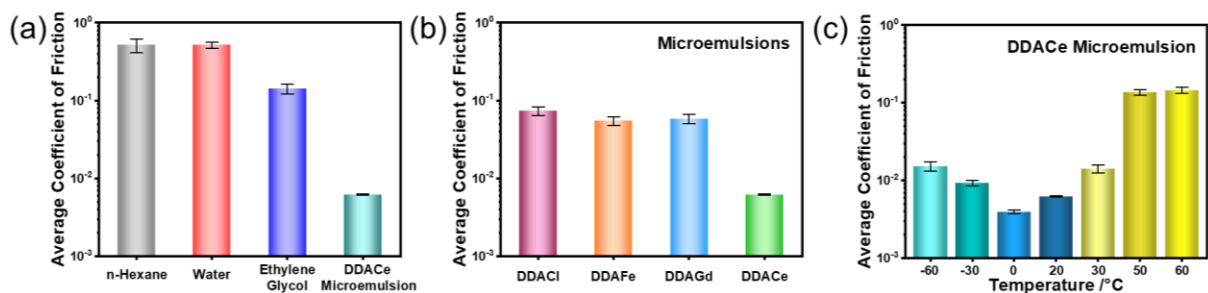
140 ● Stable MEM;

141 ⊙ Unstable MEM;

142 ○ EM;

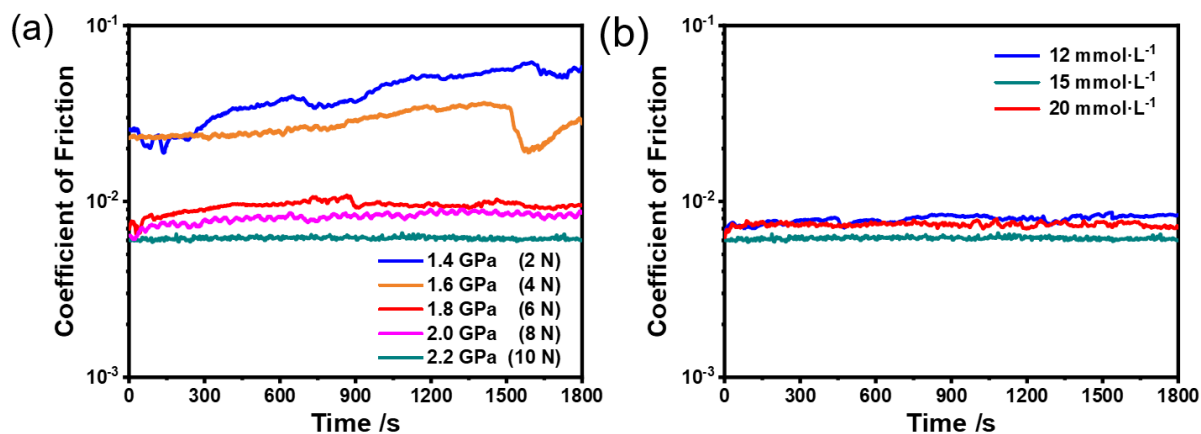
143 × No formation of EM.

144



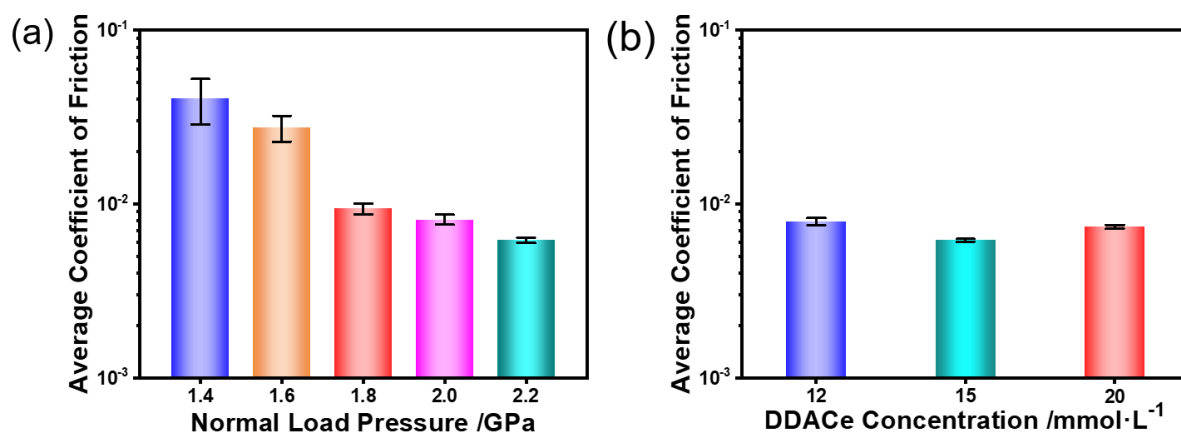
145  
 146 **Figure S7.** (a) Average CoF of n-hexane, water, EG and DDACe MEM at room temperature.  
 147 (b) Average CoF of MEM prepared with different surfactants at 20 °C. (b) Average CoF of  
 148 DDACe MEM in a temperature range from -60 to 60 °C. All the MEM (or EM) were constituted  
 149 of 35.43 wt% surfactant solution, 26.03 wt% EG and 38.54 wt% n-hexane, a constant surfactant  
 150 concentration of 15 mmol L<sup>-1</sup> and a volume ratio of water-to-oil = 1:1.

151



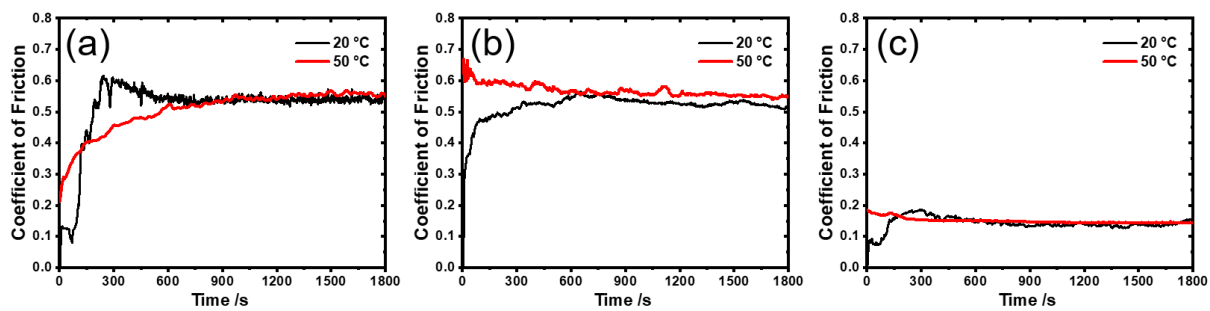
152  
 153 **Figure S8.** Effect of (a) applied normal load pressure (or normal load) and (b) surfactant  
 154 concentration on the CoF of a DDACe MEM (containing 35.43 wt% DDACe solution, 26.03  
 155 wt% EG and 38.54 wt% n-hexane,  $c_{\text{DDACe}} = 15 \text{ mmol L}^{-1}$ ,  $v_{\text{water}}:v_{\text{oil}} = 1:1$ ).  $T = 20 \text{ }^{\circ}\text{C}$ .

156



157  
 158 **Figure S9.** Average CoF of a DDACe MEM (consisting of 35.43 wt% DDACe solution, 26.03  
 159 wt% EG and 38.54 wt% n-hexane,  $c_{DDACe} = 15 \text{ mmol L}^{-1}$ ,  $v_{water}:v_{oil} = 1:1$ ) at different normal  
 160 load pressures (a) and surfactant concentrations (b).  $T = 20 \text{ }^{\circ}\text{C}$ .

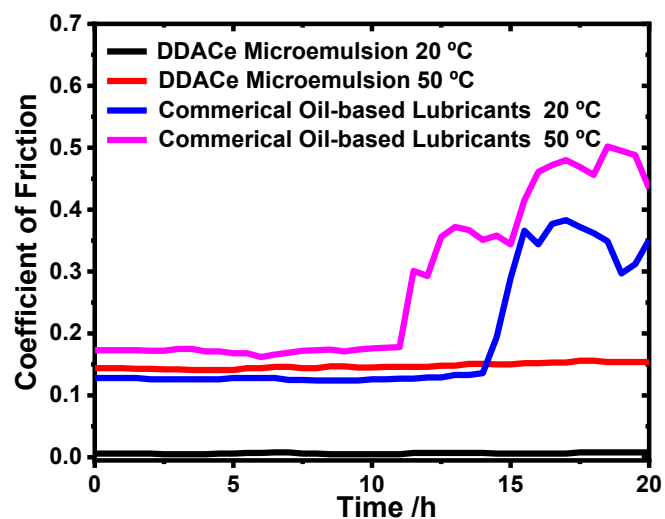
161



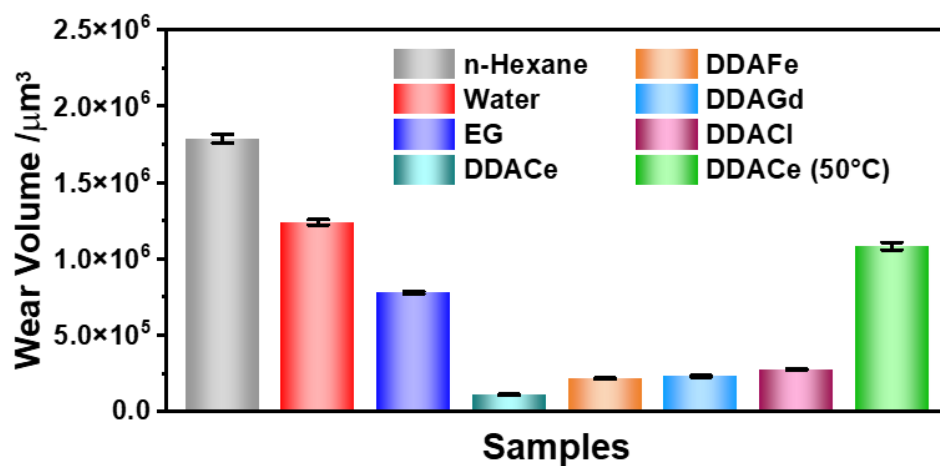
162  
163 **Figure S10.** CoF of (a) n-hexane, (b) water and (c) EG at 20 and 50 °C under an applied normal  
164 load pressure of 2.2 GPa (*i.e.*, 10 N normal load) and sliding velocity of 0.1 m s<sup>-1</sup>.

165

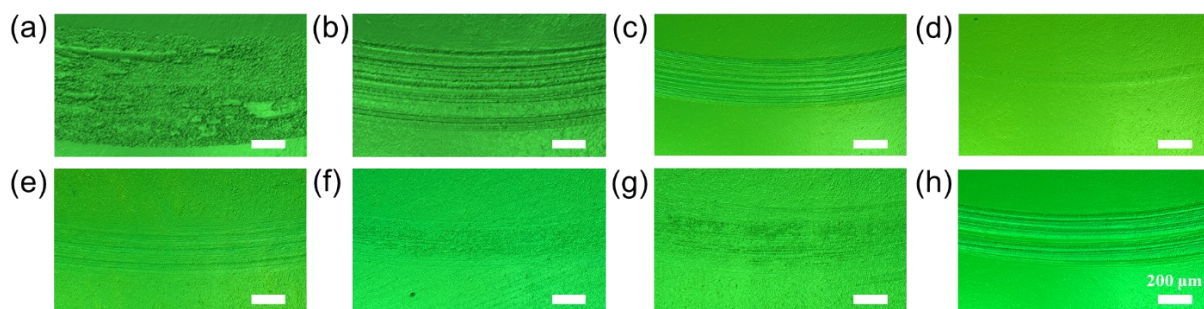




166  
 167 **Figure S11.** Comparison in the CoF between DDACe microemulsion and a commercially  
 168 available general-purpose oil-based lubricants (a mixture consisting of liquid paraffin and  
 169 additives) during a continuous measurement for 20 h at 20 and 50 °C. The applied normal load  
 170 pressure was 2.2 GPa (*i.e.*, 10 N normal load) and the sliding velocity was 0.1 m s<sup>-1</sup>.  
 171



172  
 173 **Figure S12.** Wear volume of steel substrates after lubricated with n-hexane, water, EG and  
 174 MEM (or EM) stabilized by different surfactants.  
 175



176

177 **Figure S13.** Surface topography of steel substrates after lubricated with (a) n-hexane, (b) water,

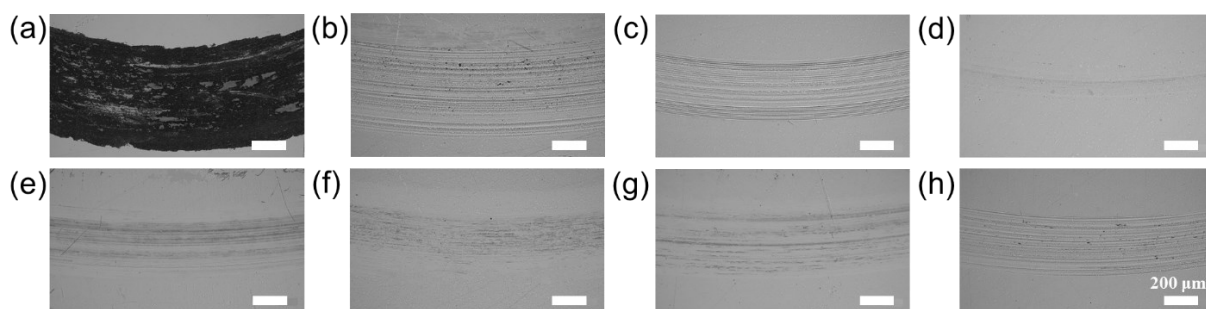
178 (c) EG, (d) DDACe MEM, (e) DDAFe MEM, (f) DDAGd MEM, (g) DDACl MEM and (h) 50

179 °C DDACe EM using 3D surface profilometer. All the MEM (or EM) contained 35.43 wt%

180 surfactant solution, 26.03 wt% EG and 38.54 wt% n-hexane, a constant surfactant concentration

181 of  $15 \text{ mmol L}^{-1}$  and a volume ratio of water-to-oil = 1:1.

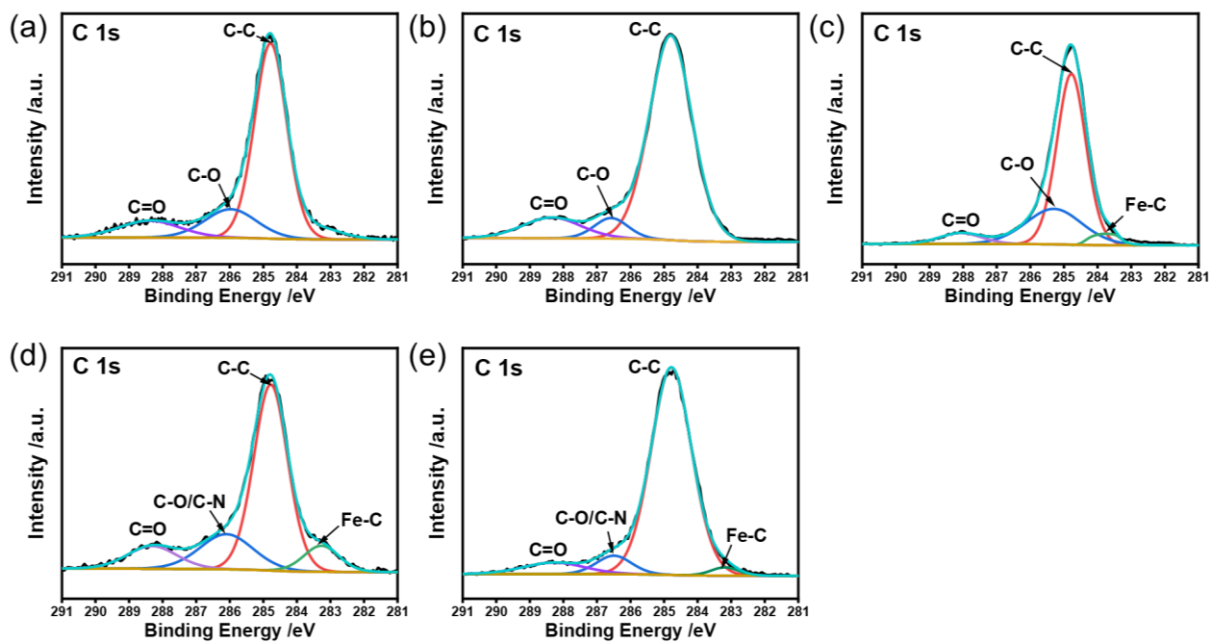
182



183

184 **Figure S14.** Optical micrographs of steel substrates after lubricated with (a) n-hexane, (b) water,  
185 (c) EG, (d) DDACe MEM, (e) DDAFe MEM, (f) DDAGd MEM, (g) DDACl MEM and (h) 50  
186 °C DDACe EM. All the MEM (or EM) were constituted of 35.43 wt% surfactant solution, 26.03  
187 wt% EG and 38.54 wt% n-hexane, a constant surfactant concentration of 15 mmol L<sup>-1</sup> and a  
188 volume ratio of water-to-oil = 1:1.

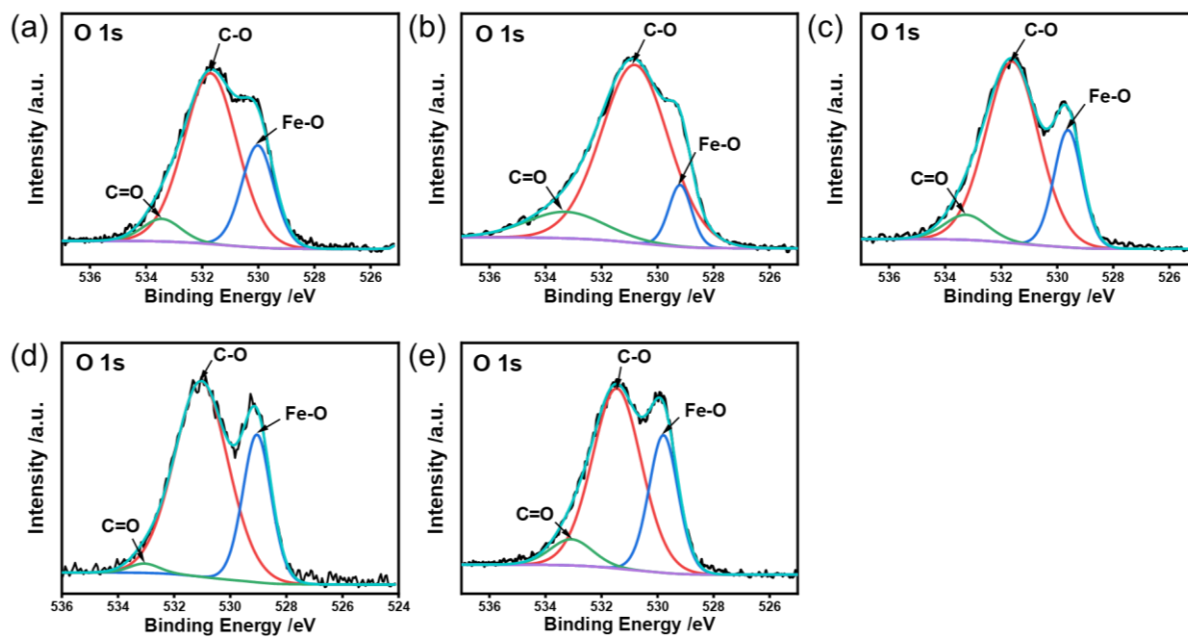
189



190

191 **Figure S15.** XPS C 1s spectra of (a) n-hexane, (b) water, (c) EG, (d) DDACe MEM and (e) 50  
 192 °C DDACe EM. All the MEM (or EM) were constituted of 35.43 wt% DDACe solution, 26.03  
 193 wt% EG and 38.54 wt% n-hexane, a constant DDACe concentration of 15 mmol L<sup>-1</sup> and a  
 194 volume ratio of water-to-oil = 1:1.

195



196

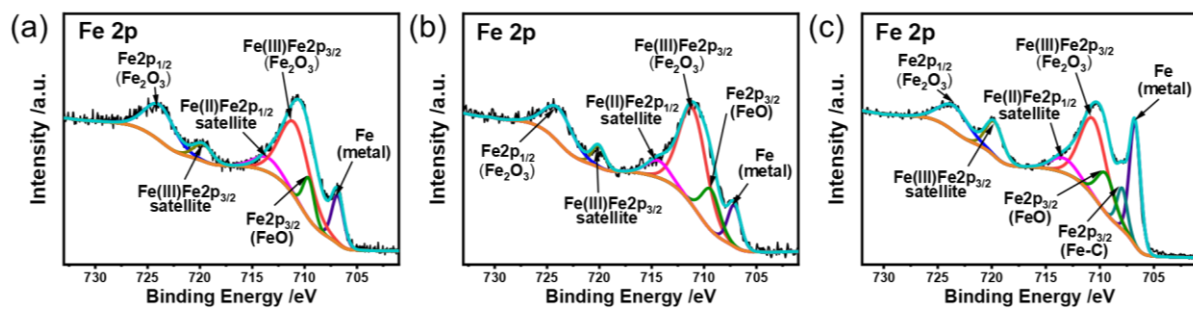
197 **Figure S16.** XPS O 1s spectra of (a) n-hexane, (b) water, (c) EG, (d) DDACe MEM and (e) 50

198 °C DDACe EM. All the MEM (or EM) consisted of 35.43 wt% DDACe solution, 26.03 wt%

199 EG and 38.54 wt% n-hexane, a constant DDACe concentration of 15 mmol L<sup>-1</sup> and a volume

200 ratio of water-to-oil = 1:1.

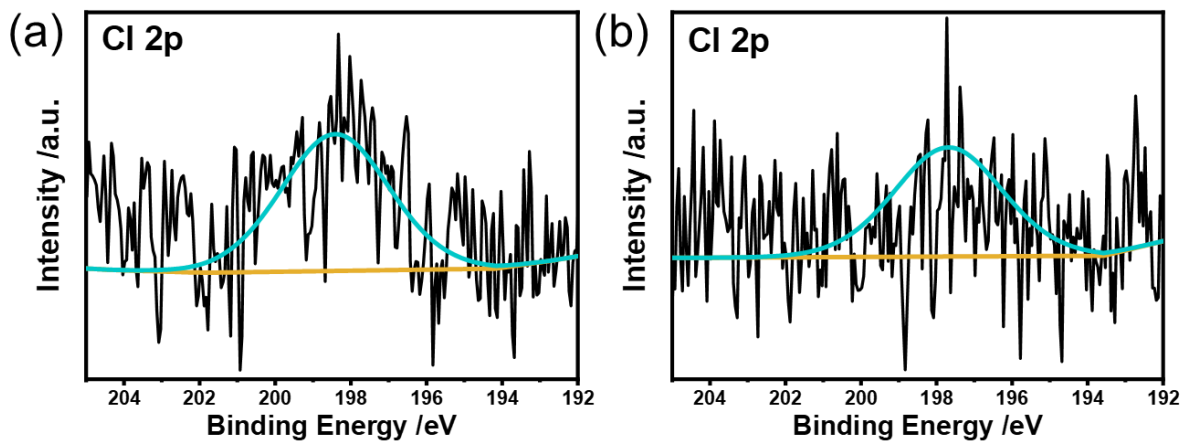
201



202

203 **Figure S17.** Additional XPS Fe 2p spectra of (a) n-hexane, (b) water and (c) EG.

204

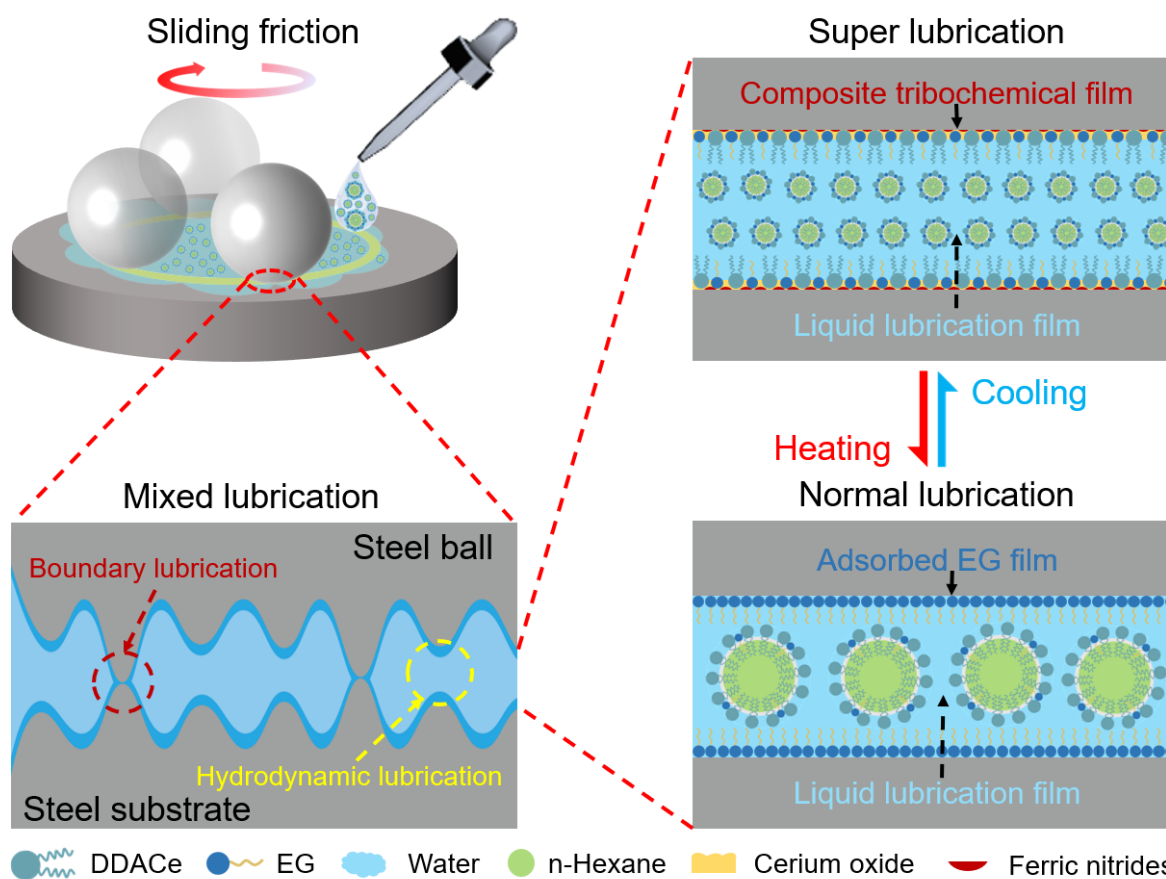


205

206 **Figure S18.** XPS Cl 2p spectra of (a) DDACe MEM and (b) 50 °C DDACe EM. Both the MEM  
207 and EM consisted of 35.43 wt% DDACe solution, 26.03 wt% EG and 38.54 wt% n-hexane, a  
208 constant DDACe concentration of 15 mmol L<sup>-1</sup> and a volume ratio of water-to-oil = 1:1.

209



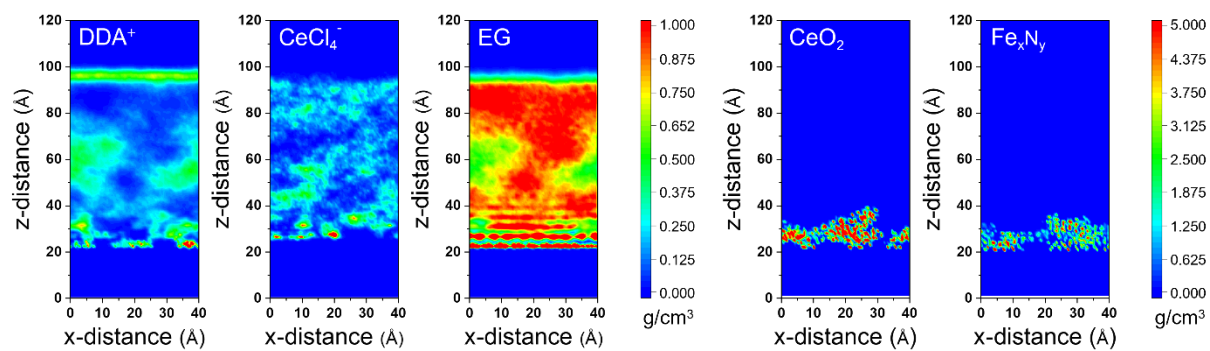


210

211 **Figure S19.** Schematic illustration of possible mechanism for thermally responsive

212 superlubrication of the DDACe/EG/n-hexane/water mixture.

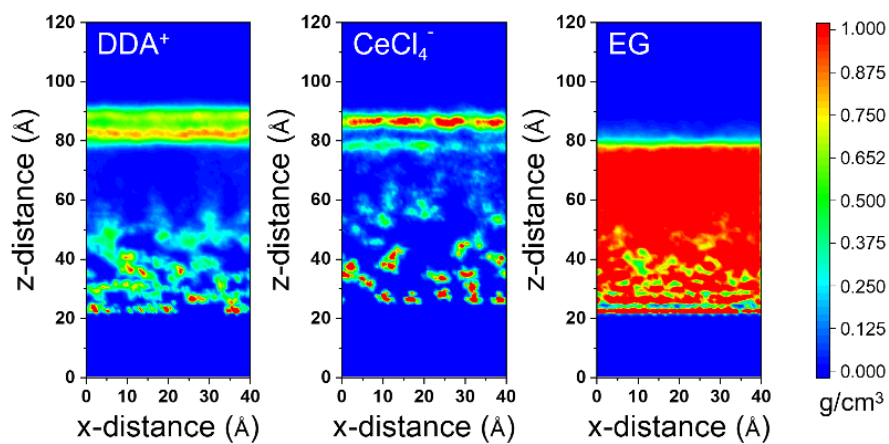
213



214

215 **Figure S20.** 2D density profiles of the DDACe/EG mixture and its tribochemical products in  
 216 the MD box at 20 °C. The scale bar indicates the density of different compounds in the studying  
 217 distance range.

218



219

220 **Figure S21.** 2D density profiles of the DDACe/EG mixture in the MD box at 50 °C. The scale

221 bar indicates the density of different compounds in the studying distance range.

222

### 223 S3: Supplementary Text

#### 224 Calculation of The Thickness of Liquid Lubrication Films

225 The thickness of liquid lubricating films between the two contacting steel surfaces was  
226 calculated according to the Hamrock-Dowson formula:<sup>7,8</sup>

$$227 \quad H_c^* = \frac{h_c}{R_x} = 2.69 \frac{G^{*0.53} U^{*0.67}}{W^{*0.067}} (1 - 0.61e^{-0.73k}) \quad (\text{Eq. S1})$$

$$228 \quad G^* = \alpha E \quad (\text{Eq. S2})$$

$$229 \quad W^* = \frac{w}{ER_x^2} \quad (\text{Eq. S3})$$

$$230 \quad U^* = \frac{\eta u}{ER_x} \quad (\text{Eq. S4})$$

$$231 \quad \frac{2}{E} = \frac{1-\mu_1^2}{E_1} + \frac{1-\mu_2^2}{E_2} \quad (\text{Eq. S5})$$

$$232 \quad k = 1.03 \left( \frac{R_x}{R_y} \right)^{0.64} \quad (\text{Eq. S6})$$

$$233 \quad \frac{d}{2} = \left( \frac{3Rw}{4E} \right)^{\frac{1}{3}} \quad (\text{Eq. S7})$$

$$234 \quad R = \frac{Ed^3}{6w} \quad (\text{Eq. S8})$$

235 Here  $H_c^*$  and  $h_c$  are the dimensionless and dimensional central film thickness, respectively;  
236  $G^*$  and  $E$  are the dimensionless and equivalent elastic moduli, respectively;  $\alpha$  ( $4 \text{ GPa}^{-1}$ ) refers  
237 to the viscosity-pressure coefficient of lubricants;  $W^*$  and  $w$  (10 N) are the dimensionless and  
238 dimensional loads, respectively;  $U^*$  and  $u$  ( $0.10 \text{ m s}^{-1}$ ) represent the dimensionless and  
239 dimensional sliding velocity;  $\eta$  (90 mPa·s at 20 °C and 138 mPa·s at 50 °C) is the viscosity of  
240 the liquid lubricants.  $\mu_1$  (0.3) and  $E_1$  (206 GPa) are the Poisson's ratio and elastic modulus for  
241 the steel ball, while  $\mu_2$  (0.3) and  $E_2$  (206 GPa) are the Poisson's ratio and elastic modulus for  
242 the steel disc.  $k$  is the ellipticity. According to the Hertzian contact theory (Eq. S7), the  
243 equivalent radius ( $R$ ) of a steel ball can be calculated from the diameter of a wear scar (112  $\mu\text{m}$   
244 at 20 °C and 239  $\mu\text{m}$  at 50 °C) using Eq. S8, i.e.,  $R=R_x=R_y$  (5.3 mm at 20 °C and 51.3 mm at

245 50 °C) DDACe EM. As a consequence, the thickness of liquid films between the tribopair was  
246 calculated to be ~32 nm for DDACe MEM at 20 °C and ~123 nm for DDACe EM at 50 °C.

247 The thickness-roughness ratio ( $\lambda$ ) of liquid lubrication films was further calculated to  
248 probe the physical lubricating mechanism of MEM or EM lubricants:

$$249 \quad \lambda = \frac{h_c}{\sqrt{\sigma_1^2 + \sigma_2^2}} \quad (\text{Eq. S9})$$

250 Where  $\sigma_1$  (18 nm at 20 °C and 32 nm at 50 °C) and  $\sigma_2$  (18 nm at 20 °C and 32 nm at 50 °C)  
251 are the surface roughness of a worn steel ball and disc, respectively. The lubrication nature can  
252 be evaluated according to: 1)  $\lambda < 1$  for boundary lubrication; 2)  $1 \leq \lambda \leq 3$  for mixed lubrication; and  
253 3)  $\lambda > 3$  for hydrodynamic lubrication, respectively.

254

255 **References**

- 256 1. P. Brown, A. Bushmelev, C. P. Butts, J. Cheng, J. Eastoe, I. Grillo, R. K. Heenan and  
257 A. M. Schmidt, *Angew. Chem. Int. Ed.*, 2012, **51**, 2414-2416.
- 258 2. S. Chen, J. Wang, H. Lu and L. Xu, *ACS Sustainable Chem. Eng.*, 2022, **10**, 10816-  
259 10826.
- 260 3. L. Wang and X. Liu, *Wear*, 2013, **304**, 13-19.
- 261 4. X. Liu, L. Wang and Q. Xue, *Tribol. Int.*, 2013, **60**, 36-44.
- 262 5. H. Sun, S. J. Mumby, J. R. Maple and A. T. Hagler, *J. Am. Chem. Soc.*, 1994, **116**, 2978-  
263 2987.
- 264 6. K. Kanhaiya, S. Kim, W. Im and H. Heinz, *npj Compt. Mater.*, 2021, **7**, 17.
- 265 7. D. Dowson and G. R. Higginson, *Elasto-hydrodynamic lubrication: international series*  
266 *on materials science and technology*, Elsevier, 2014.
- 267 8. D. Dowson and G. Higginson, *Elasto-Hydrodynamic Lubrication*, 1977, 20-29.  
268